Journal of Solid State Chemistry 183 (2010) 1309–1313

Contents lists available at ScienceDirect

Journal of Solid State Chemistry

journal homepage: www.elsevier.com/locate/jssc

Crystal structure investigations of $ZrAs_xSe_y$ ($x > y$, $x+y \leq 2$) by single crystal neutron diffraction at 300 K, 25 K and 2.3 K

Rainer Niewa [a,*], Andreas Czulucki [b], Marcus Schmidt [b], Gudrun Auffermann [b], Tomasz Cichorek [c], Martin Meven [d], Björn Pedersen [d], Frank Steglich [b], Rüdiger Kniep [b]

[a] Institut für Anorganische Chemie, Universität Stuttgart, Pfaffenwaldring 55, 70569 Stuttgart, Germany
[b] Max-Planck-Institut für Chemische Physik fester Stoffe, Nöthnitzer Straße 40, 01187 Dresden, Germany
[c] Institute of Low Temperature and Structure Research, ul. Okólna 2, 50-442 Wroclaw, Poland
[d] Forschungsneutronenquelle Heinz Maier-Leibnitz (FRM II), Lichtenbergstraße 1, Technische Universität München, 85747 Garching, Germany

ARTICLE INFO

Article history:
Received 19 February 2010
Received in revised form
1 April 2010
Accepted 4 April 2010
Available online 9 April 2010

Keywords:
Arsenide
Selenide
Zirconium
PbFCl type structure
Neutron diffraction

ABSTRACT

Large single crystals of $ZrAs_xSe_y$ ($x>y$, $x+y \leq 2$, PbFCl type of structure, space group $P4/nmm$) were grown by Chemical Transport. Structural details were studied by single crystal neutron diffraction techniques at various temperatures. One single crystal specimen with chemical composition $ZrAs_{1.595(3)}Se_{0.393(1)}$ was studied at ambient temperature ($R1=5.10$ %, $wR2=13.18$ %), and a second crystal with composition $ZrAs_{1.420(3)}Se_{0.560(1)}$ was investigated at 25 K ($R1=2.70$%, $wR2=5.70$ %) and 2.3 K ($R1=2.30$ %, $wR2=4.70$ %), respectively. The chemical compositions of the crystals under investigation were determined by wavelength dispersive X-ray spectroscopy. The quantification of trace elements was carried out by Laser Ablation–Inductively Coupled Plasma–Mass Spectrometry. According to the crystal structure refinements the crystallographic 2*a* site is occupied by As, together with a significant amount of vacancies. One of the 2*c* sites is fully occupied by As and Se (random distribution). With respect to the fractional coordinates of the atoms, the crystal structure determinations based on the data obtained at 25.0 K and 2.3 K did not show significant deviations from ambient temperature results. The temperature dependence of the displacement parameters indicates a static displacement of As on the 2*a* sites (located on the (0 0 1) planes) for all temperatures. No indications for any occupation of interstitial sites or the presence of vacancies on the Zr (2*a*) site were found.

1. Introduction

The low-temperature behaviour of the electrical resistivity of ferromagnetic UAsSe and the diamagnetic counterpart ThAsSe is apparently governed by an interaction of the conduction-electrons with dynamical defects of non-magnetic origin [1–3]. Recently, we have observed a similar effect for $ZrAs_{1.4}Se_{0.5}$ [4–7] and $HfAs_{1.7}Se_{0.2}$ [8], i.e., a magnetic-field-independent–$AT^{1/2}$ term in the electrical resistivity below 16 K. Thus, this class of compounds displays signatures characteristic for a non-magnetic Kondo effect, possibly due to the presence of defects in the crystal structure [9]. All these compounds crystallize in an undistorted tetragonal PbFCl type of structure. In this structure type the larger anions typically occupy a 2*c* site while the smaller anions are located on the 2*a* site. However, the anions may principally be distributed among both sites in the sense of substitution. In case of $ZrAs_{1.40}Se_{0.50}=ZrAs_{0.90(1)}(Se_{0.50(1)}As_{0.50})$, the 2*c* site is fully occupied by As/Se with random occupation, and a deficiency in the arsenic layer (site 2*a*) is observed [4]. Nevertheless, it is hardly possible to distinguish between As and Se from standard X-ray diffraction data, due to the only one-electron difference. This means, that in principle several order/disorder variants of As and Se as well as vacancies or occupation of interstitial positions might be discussed. Here, we present neutron diffraction data obtained from two single crystals with different chemical compositions $ZrAs_xSe_y$, but close to $Zr(As,Se)_2$, in order to analyse the As–Se-distribution over the two crystallographic non-metal sites. Since the unusual transport properties become effective only at temperatures below 20 K, one may speculate about phase transitions or even more subtle crystallographic changes at low temperatures. No low-temperature diffraction data are reported so far. Therefore, we have refined the crystallographic data from neutron diffraction measurements at 25 K and at 2.3 K in order to address these open points.

2. Experimental

2.1. Synthesis

Crystals up to $5 \times 4 \times 4\,mm^3$ in size were synthesized from Zr (Goodfellow, 99.2 wt.%, powder, content of Hf: 2500 ppm),

* Corresponding author. Fax: +49 711 685 64241.
E-mail address: rainer.niewa@iac.uni-stuttgart.de (R. Niewa).

0022-4596/$ - see front matter © 2010 Elsevier Inc. All rights reserved.
doi:10.1016/j.jssc.2010.04.006

As (Chempur, 99.999 wt.%), and Se (Chempur, 99.999 wt.%) by an exothermal Chemical Transport Reaction in a temperature gradient from 1123 K (source) to 1223 K (sink) [6]. As the reactants may attack the fused silica container material, which then leads to silicon contamination of the products, we inserted a glassy carbon tube into the fused silica ampoule. By using a pre-reacted mixture of the elements with the molar ratio n(Zr): n(As): n(Se)=1: 1: 1 we succeeded in growing single crystals with high As and low Se content resulting in general compositions close to $Zr(As,Se)_2$.

2.2. Characterization

2.2.1. X-ray powder diffraction

For X-ray powder diffraction experiments finely ground crystals were investigated in a transmission set-up using an Imaging Plate Guinier Camera (HUBER 670, Co$K\alpha_1$ radiation, 4×15 min scans, $8^\circ\le2\theta\le100^\circ$). Low temperatures were generated by applying a He cryostat. Seven patterns were taken in the temperature range from ambient temperature to 20 K. The unit cell parameters were refined by least-squares fittings of the X-ray powder data (CSD program package [10]) with LaB_6 (a=415.692(1) pm) as internal standard. The chemical composition of the sample used was $Zr_{1.00(1)}As_{1.39(1)}Se_{0.59(1)}$ (see below).

2.2.2. Single crystal neutron diffraction at ambient temperature

A single crystal with approximate edge sizes of $2\times2\times2$ mm^3 (crystal I) was measured on the single crystal diffractometer RESI at FRM-II (Reciprocal Space Investigator, thermal source, Garching, Germany) at ambient temperature with 180° ϕ-scans (step width 1°, 640 s/frame) at θ=15°, −22.5°, −35°, −45° and a 40° Ω-scan at $\theta=-20^\circ$ with $\chi=90^\circ$. A detailed description of the set-up including the kappa goniometer, the Cu-422 monochromator and the neutron sensitive imaging plate can be found elsewhere [11]. The images were binned (3×3) and integrated with the software package *EVAL*14 [12]. Cell refinements were carried out with the program *peakref* (Bruker-Nonius, Delft). The final cell parameter refinements from 163 reflections gave a tetragonal ($4/m$) unit cell with a=378.30(7) pm, c=813.6(1) pm and $V=116.44\times10^6$ pm^3. Due to the higher accuracy, in the following we use the unit cell parameters obtained from X-ray powder diffraction data (a=375.76(2) pm, c=807.80(5) pm). 462 reflections were integrated, 158 of which were unique, and 49 had only weak intensity ($I/\sigma(I)<2$). 27 negative and 31 reflections with poor background quality were omitted from the final data set (R_{sym}=0.044, R_{meas}=0.051, χ^2=8.369, I(mean)=149.637 counts, No.(unique reflections)=136, No.(reflections)=355). Extinction correction was carried out in the isotropic Gaussian Type I-model. Neutron scattering lengths used in the refinements: b_c(Zr)=7.16 fm, b_c(As)=6.58 fm, b_c(Se)=7.97 fm [13].

2.2.3. Single crystal neutron diffraction at low temperatures

A second single crystal (crystal II) with similar shape as crystal I and approximate edge sizes of $1.5\times1.5\times1.5$ mm^3 originating from a different Chemical Transport experiment was measured at the single crystal diffractometer HEiDi at FRM-II (Heißes Einkristalldiffraktometer, hot source, Garching, Germany) at 25.0 K and 2.3 K. A short wavelength of 55.2(1) pm combined with a high flux density of $>2\times10^6$ neutrons per second and cm^2 was obtained using a Cu-(4 2 0) monochromator yielding a comparably large available q-space. Low-temperatures were realized by a He closed-cycle cryostat mounted in the Eulerian cradle of the diffractometer. The sample crystal was wrapped in Al foil to ensure temperature homogeneity. The temperature was measured and controlled by a diode sensor near the heater position and a stability of ±0.1 K was achieved. The absolute temperatures were measured by an additional temperature sensor at the sample position. The corrected integrated intensities of the reflections were calculated using the program *PRON2 K* [14], numerical absorption correction was performed with the program *TBAR* [15]. Details on the diffractometer set-up can be found in literature [16].

The unit cell was determined at 2.3 K (a=375.0(3) pm, c=803.7(1) pm). These parameters were also used for the data collection at 25.0 K. At 25.0 K (2.3 K) 1679 (1518) reflections were measured, 1242 (1142) of which were above $I/\sigma(I)<2$.

All structure refinements (crystals I and II) were carried out using the program *SHELXL-97-2* [17] starting with the structural model derived from X-ray diffraction data [4] (unit cell parameters from powder XRD: a=375.86(2) pm, c=805.45(7) pm). Structure refinements in any other space group than the selected *P*4/*nmm* did not lead in any noteworthy improvement of the structural model. No significant intensities associated with diffuse scattering were observed in any experiment.

2.2.4. Determination of chemical composition

As was shown already in a recent publication [6] the results of chemical analysis and WDXS are in good agreement. For WDXS (CAMECA SX 100) investigations, fragments of crystals I and II (after being used for neutron diffraction) were embedded coplanar to well-formed prism faces and processed metallographically. The WDXS system was calibrated by use of a ternary Zr–As–Se standard crystal. Further elements as possible impurities, such as silicon were not detected by WDXS (limit of detection: 0.5 at.%). The WDXS-analyses resulted in the chemical composition $ZrAs_{1.595(3)}Se_{0.393(1)}\equiv Zr(As,Se)_{1.988(4)}$ for crystal I and $Zr_{1.000(2)}As_{1.420(3)}Se_{0.560(2)}\equiv Zr(As,Se)_{1.980(4)}$ for crystal II, respectively.

2.2.5. Determination of trace element impurities

In earlier studies, particularly Si impurities stemming from the fused silica tube as well as small amounts of Fe accounted for some difficulties. For quantification of traces of Si and Fe (Laser Ablation–Inductively Coupled Plasma–Mass Spectrometry, LA–ICP–MS) a new sample was prepared by an identical Chemical Transport Reaction leading to crystals with chemical compositions closely related to crystals I and II according to WDXS analyses. The measurements were carried out with the laser ablation system Geoloas Q Plus (Coherent) connected with an ICP–MS 800 (Varian). For detailed description of the method and principles of the measurements see Refs. [18,19]. In the present work a 193 nm ArF eximer laser was used at a pulse repetition rate of 5 Hz, 5 J/cm^2 to ensure a controlled sample uptake. The diameter of the laser spot was 50 microns. Five individual ablations were carried out on five crystals each resulting in basically identical concentrations for both trace impurities with an average of w(Si)=0.14 ± 0.02 wt.% and w(Fe)=0.21 ± 0.02 wt.%. Thus, both impurities should not lead to major problems in the data interpretation.

3. Results and discussion

As demonstrated earlier the arsenic-rich phase $ZrAs_xSe_y$ exists in a narrow homogeneity triangle ($1.38\ (1)\le x\le1.65(1)$; $0.32(1)\le y\le0.61(1)$; $1.90(1)\le(x+y)\le1.99(1)$) at 1223 K [6]. Fig. 1 shows the respective isothermal section of the ternary system. Crystal specimens from the homogeneity range crystallize in the tetragonal PbFCl type of structure (space group *P*4/*nmm*). Fig. 2 exemplifies an image of single crystal II used for neutron diffraction and subsequently for the determination of the

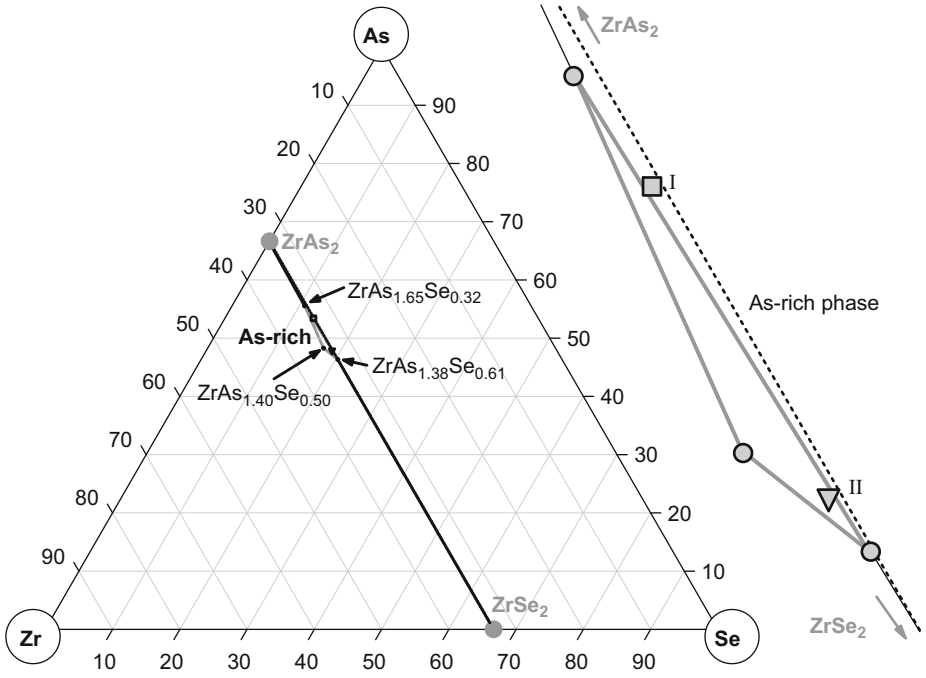

Fig. 1. Isothermal section of the ternary system Zr–As–Se at 1223 K: the chemical compositions $ZrAs_{1.595(3)}Se_{0.393(1)}$ (crystal I) and $ZrAs_{1.420(3)}Se_{0.560(2)}$ (crystal II) are marked by a square and a triangle, respectively.

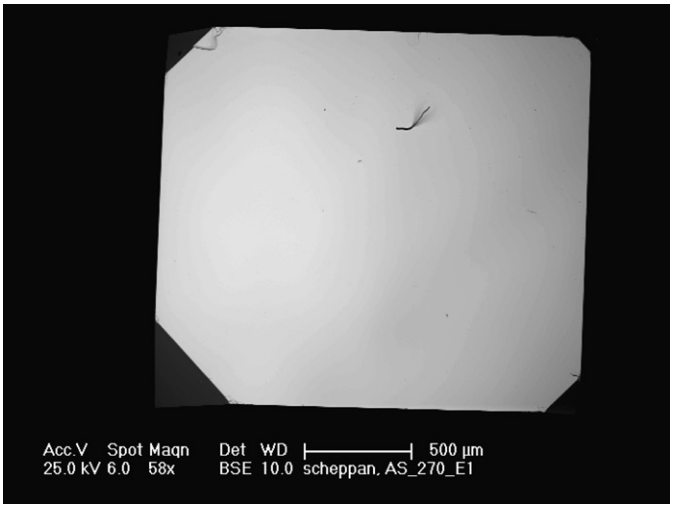

Fig. 2. Crystal II (SEM image, $ZrAs_{1.420(3)}Se_{0.560(2)}$) used for single crystal neutron diffraction.

chemical composition. Crystal I was used for ambient temperature neutron diffraction. The chemical composition from WDXS analyses, $Zr_{1.000(3)}As_{1.595(3)}Se_{0.393(1)}$, demonstrates a composition close to $Zr(As,Se)_2$ (with a small number of vacancies in the anionic substructure). An X-ray single crystal diffraction experiment on a fragment of the crystal resulted in the chemical formula $Zr(As,Se)_{1.974(2)}$, which is in excellent agreement with the general composition of $Zr(As,Se)_{1.988(4)}$ obtained from WDXS analysis. Crystal II ($Zr_{1.000(2)}As_{1.420(3)}Se_{0.560(2)}$) was used for neutron diffraction at low temperatures. Fig. 1 illustrates the chemical compositions of both crystals within the homogeneity range. It should be noted, that the tie line between $ZrAs_2$ and $ZrSe_2$ does not cross the homogeneity range, that is, the crystalline phase under consideration exists only with a minimum of deviation from $Zr(As,Se)_2$. According to all our experimental data this deviation $Zr(As,Se)_{2-\delta}$ is realized via vacancies within the non-metal substructure, rather than by interstitial Zr-atoms ($\delta=2-(x+y)$ in $ZrAs_xSe_y$).

In agreement with our previous studies [4,5] the refinements of the single crystal neutron diffraction data show that the non-metal deficit occurs on the crystallographic 2*a* site rather than on the 2*c* site. Tables 1 and 2 gather crystallographic data and information on data collection. The presented data indicate that the 2*a* site is occupied by arsenic, while the 2*c* site is mixed occupied by As and Se: In case of crystal I that means 60% As and 40% Se. In order to ascertain this result, the refinements of the neutron diffraction data in several independent runs were performed with occupation of both sites either fully with As, fully with Se, or partly with As and Se, respectively. The preferred model resulted in the best refinement as indicated by the lowest reliability factors, the most reasonable displacement factors of all atoms and the closest refined composition as compared with the results from the WDXS analyses. The refinements of the data obtained from crystal I converged with a composition of $ZrAs_{0.96(2)}(As_{0.52(8)}Se_{0.48})=ZrAs_{1.48(10)}Se_{0.48}$ which equals the composition obtained from WDXS analysis within the standard deviations. An alternative fixed occupation of the 2*c* site with 60% As and 40% Se according to the WDXS analysis hardly changed the quality of the refinements. Therefore, in the following we assign crystal I the chemical composition observed by WDXS analyses. The alternative occupation of the 2*a* site with 60% As and 40% Se and a 2*c* site purely occupied by As led to significantly higher reliability factors and to large displacement parameters. This clearly demonstrates the correctness of the assignment of the site occupations according to Table 2 and Fig. 3.

Similar conclusions can be drawn from the data for crystal II measured at 25.0 K and 2.3 K, respectively. The refinement of the data obtained at 25.0 K resulted in the chemical compositions $ZrAs_{0.980(4)}(As_{0.38(2)}Se_{0.62})=ZrAs_{1.36(2)}Se_{0.62}$, and at 2.3 K in $ZrAs_{0.975(4)}(As_{0.35(2)}Se_{0.65})=ZrAs_{1.33(2)}Se_{0.65}$. This is in reasonable agreement with the analytical composition $Zr_{1.000(2)}As_{1.420(3)}Se_{0.560(2)}$ (WDXS).

Table 1
Crystal data and structure refinement details for $Zr_{1.000(3)}As_{1.595(3)}Se_{0.393(1)}$ and $Zr_{1.000(2)}As_{1.420(3)}Se_{0.560(2)}$.

Specimen		Crystal I		Crystal II[a]	
Chemical composition (WDXS)		$Zr_{1.000(3)}As_{1.595(3)}Se_{0.393(1)}$		$Zr_{1.000(2)}As_{1.420(3)}Se_{0.560(2)}$	
Crystal dimensions/mm		$2 \times 2 \times 2$		$1.5 \times 1.5 \times 1.5$	
Temperature/K		300		25.0(1)	2.3(1)
Radiation		Neutron		Neutron	
Diffractometer		RESI		HEiDi	
Wavelength/pm		104.9(1)		55.2(1)	
Space group		P4/*nmm*		P4/*nmm*	
Z		2		2	
Cell dimensions	*a*	378.30(7)		375.0(3)	
Neutron/pm	*c*	813.6(1)		803.7(1)	
$V/10^6$ pm^3		116.44		113.02	
Cell dimensions	*a*	375.76(2)		375.86(2)	
X-ray/pm	*c*	807.80(5)		805.45(7)	
$2\theta_{max}$/deg		110.8		75.0	
hkl range		± 4	−6–+8		–6–+7
		−4– +3	–3–+8		–3–+7
		± 12	–17–+16		± 16
No. reflections		355	1679		1518
No. parameter		12	12		12
GOF		1.26	1.09		1.14
*R*1/*wR*2		0.051/0.132	0.027/0.057		0.023/0.047
Largest difference peak		0.74	0.97		0.96
Refined composition		$ZrAs_{1.48(10)}Se_{0.48}$	$ZrAs_{1.36(2)}Se_{0.62}$		$ZrAs_{1.33(2)}Se_{0.65}$

[a] The unit cell was determined at 2.3 K. These parameters were also used for the data collection at 25.0 K since the accuracy of the unit cell determination with the neutron diffraction set-up is low.

Table 2
Fractional coordinates and displacement parameters.

Atom	Site	*x*	*y*	*z*	U_{11}	U_{33}	U_{eq}	occ.
Zr	2*c*	$^1/_4$	$^1/_4$	0.2666(2)	0.0062(6)	0.0072(7)	0.0065(5)	1
				0.26505(3)	0.00247**(7)**	**0.00181(7)**	**0.00225(6)**	
				0.26506(2)	*0.00237(7)*	*0.00176(7)*	*0.00217(6)*	
As	2*a*	$^3/_4$	$^1/_4$	0	0.0089(8)	0.0072(8)	*0.0083(7)*	0.96(2)
					0.00671(9)	**0.00204(8)**	**0.00515(7)**	**0.979(4)**
					0.00644(8)	*0.00193(8)*	*0.00494(7)*	*0.975(4)*
As/Se	2*c*	$^1/_4$	$^1/_4$	0.6205(2)	0.0058(6)	0.0077(7)	*0.0065(5)*	0.52(8)/0.48
				0.62157(2)	**0.00153(6)**	**0.00233(6)**	**0.00180(5)**	**0.38(2)/0.62**
				0.62152(2)	*0.00162(6)*	*0.00238(6)*	*0.00187(5)*	*0.35(2)/0.65*

Parameters (in 10^4 pm^2) for $ZrAs_{1.595(3)}Se_{0.393(1)}$ at ambient temperature (values in first row), and for $Zr_{1.000(2)}As_{1.420(3)}Se_{0.560(2)}$ at 25.0 K (values in bold) and at 2.3 K (values in italic). $U_{22}=U_{11}$, $U_{ij}=0$.

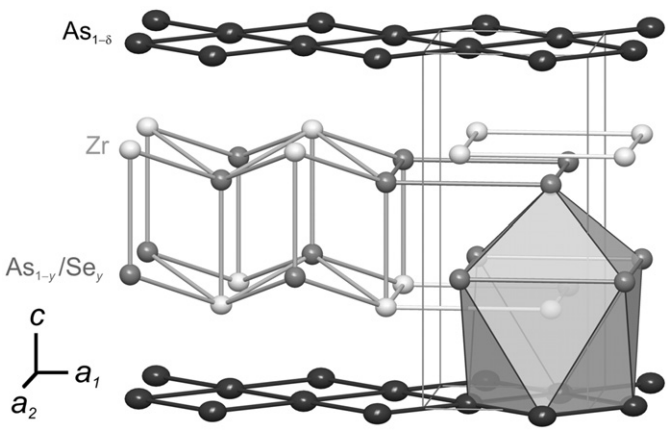

Fig. 3. Crystal structure of $ZrAs_xSe_y$ ($1.38(1) \le x \le 1.65(1)$; $0.32(1) \le y \le 0.61(1)$; $1.90(1) \le (x+y) \le 1.99(1)$):Tetrag onal PbFCl type of structure with vacancies $\delta=2-(x+y)$ on the 2*a* site (black) exclusively occupied by As, mixed occupation (As, Se) on 2*c* (grey) and a fully occupied Zr site (white).

For the correlation of chemical composition and crystal structure with the low-temperature transport properties, not only the As–Se disorder scheme is of interest, but especially the low-temperature diffraction data are of crucial importance. However, no such data have been presented so far, partly caused by the difficulties of performing X-ray diffraction experiments at defined temperatures below 10 K. The temperatures of 25.0 K and 2.3 K in the presented neutron diffraction study were selected slightly above and well below the onset-temperature of the Kondo-behaviour observed in, e.g., the electrical resistivity of $ZrAs_xSe_y$ [4]. Additionally, Fig. 4 shows the temperature dependence of the unit cell parameters from powder X-ray diffraction down to 20 K obtained from a powdered sample with similar chemical composition. These X-ray diffraction data exhibit the usually expected behaviour. Both, powder X-ray diffraction data (no indication for additional reflections or reflection splitting; constant full-width at half-maximum) as well as all neutron single crystal data give no evidence for a distortion of the crystal structure in the sense of a symmetry reduction or phase transition down to the lowest studied temperature of 2.3 K.

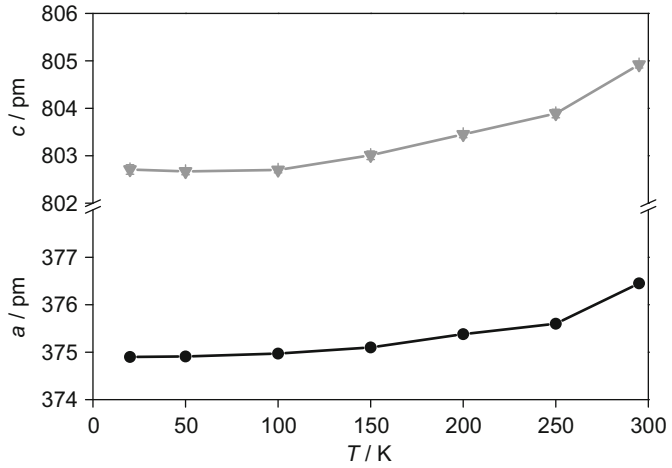

Fig. 4. Temperature dependence of unit cell parameters of a sample with chemical composition $Zr_{1.00(1)}As_{1.39(1)}Se_{0.59(1)}$ obtained from X-ray powder diffraction data (Co$K\alpha_1$-radiation). Standard deviations are below the size of the symbols.

Such distortion variants even at ambient temperatures were frequently observed for similar compounds with chemical compositions close to a 1:1:1 atomic ratio of the constituents. These comprise, e.g., formation of zig-zag chains in CeAsS [20] and GdAsSe [21], and As_2 dumbbells in NdAsSe [21]. However, even small deviations from the ideal composition may lead to a vanishing distortion from the tetragonal metric and the crystallographic symmetry of space group $P4/nmm$ [22]. All the previously investigated samples with large deviations from a 1:1:1 composition in the systems Zr–As–Se and Hf–As–Se did not reveal any indication for long range ordering and subsequent crystallographic distortion due to additional bond formation [4–6,8]. Since also the fractional coordinates of all atomic positions do not significantly change upon cooling from ambient temperature to 2.3 K (Table 2) we can exclude any static structural distortion or superstructure in the investigated temperature range and particularly in the relevant temperature range below 20 K. Additionally, the formation of local distortions without long-range periodicity upon temperature reduction, e.g. formation of covalent bonds not present at higher temperatures, should be observable in an unexpected increase of displacement parameters along the bonding directions. Again, no such observation can be taken from the refinement results given in Table 2. On the contrary, all displacement parameters diminish in the expected way upon cooling, except for the unusual large U_{11} parameter of As at site 2*a*, which stays significantly enlarged at all temperatures under investigation. The displacement parameter U_{33} for this site, describing perpendicular displacements along [0 0 1] exhibits the normal decrease with *T*. This behaviour can be taken as an indication for a static (random) displacement of As at this crystallographic site within the (0 0 1) plane, which was earlier interpreted as being due to covalent bond formation As–As without long-range order of the resulting oligomeric units [4,23,24]. Since this displacement parameter is nearly constant over the whole temperature range from ambient temperature to 2.3 K, such bond formation apparently is completed well above the onset of the unusual transport properties (compare also the physical properties discussion on this topic in [5]) and therefore should not directly be responsible for the observed physical properties at low temperatures. However, disordered As-oligomers within As-deficient layers may well provide defect centres for scattering of the conduction-electrons, as noticeable at low temperatures and described with a non-magnetic Kondo mechanism [9].

4. Conclusions

Neutron diffraction experiments performed on single crystals of $ZrAs_xSe_y$ $(x+y \approx 2)$ with chemical compositions close to $Zr(As,Se)_2$ give evidence for the As–Se-distribution in the PbFCl type crystal structure. From the two crystallographic sites for As and Se, one is occupied by both As and Se, the second one is occupied by As only. However, a noteworthy amount of defects is localized on the latter positions. No significant crystallographic changes, which might be correlated with the emerging Kondo-behaviour in, e.g., the electrical resistivity at low temperatures, occur on cooling down to 2.3 K. The temperature dependence of the displacement parameters indicates a static displacement of the pure As-site within the (0 0 1) planes, which can be interpreted as a result from disordered As-oligomers.

Acknowledgment

We would like to thank Dr. Ulrich Burkhardt, Monika Eckert, and Petra Scheppan (EDXS/WDXS analyses, metallography), Maik Böhme (LA-ICP-MS), Dr. Yurii Prots, Dr. Raúl Cardoso and Dr. Horst Borrmann (X-ray diffraction) for experimental support. Additionally, we are grateful for the beamtime assignments at FRM-II.

References

[1] T. Cichorek, H. Aoki, J. Custers, P. Gegenwart, F. Steglich, Z. Henkie, E.D. Bauer, M.P. Maple, Phys. Rev. B 68 (2003) 144411.
[2] T. Cichorek, A. Sanchez, P. Gegenwart, A. Wojakowski, Z. Henkie G. Auffermann, F. Weickert, S. Paschen, R. Kniep, F. Steglich, Phys. Rev. Lett. 94 (2005) 236603.
[3] Z. Henkie, R. Wawryk, A. Wojakowski, T. Cichorek, F. Steglich, Phys. B: Cond. Matter 378–380 (2006) 956–958.
[4] M. Schmidt, T. Cichorek, R. Niewa, A. Schlechte, Yu. Prots, F. Steglich, R. Kniep, J. Phys.: Cond. Matter 17 (2005) 5481–5488.
[5] T. Cichorek, D. Gnieda, R. Niewa, A. Schlechte, M. Schmidt, Yu. Prots R. Ramlau, Z. Henkie, R. Kniep, F. Steglich, J. Low Temp. Phys. 147 (2007) 309–319.
[6] A. Schlechte, R. Niewa, M. Schmidt, G. Auffermann, Yu. Prots, W. Schnelle D. Gnida, T. Cichorek, F. Steglich, R. Kniep, Sci. Technol. Adv. Mater. 8 (2007) 341–346.
[7] T. Cichorek, L. Bochenek, R. Niewa, M. Schmidt, A. Schlechte, R. Kniep, F. Steglich, J. Phys.: Conf. Ser. 200 (2010) 012021-1-4.
[8] A. Schlechte, R. Niewa, M. Schmidt, H. Borrmann, R. Kniep, Z. Kristallogr. NCS 222 (2007) 369–370.
[9] For a review see: D.L. Cox, A. Zawadowski, Adv. Phys. 47 (1998) 599–942.
[10] L.G. Akselrud, P.Y. Zavalii, Y.N. Grin, V.K. Pecharsky, B. Baumgartner, E. Wölfel, Mater. Sci. Forum 133–136 (1993) 335–342.
[11] B. Pedersen, F. Frey, W. Scherer, P. Gille, G. Meisterernst, Phys. B 385–386 (2006) 1046–1048.
[12] A.J.M. Duisenberg, L.M.J. Kroon-Batenburg, A.M.M. Schreurs, J. Appl. Cryst. 36 (2003) 220–229.
[13] International Tables for Crystallography, Vol. C, 3rd ed., E. Prince (Ed.), Kluwer, Dordrecht, 2004.
[14] Program for Data Reduction of DIF4. Version of Institut für Kristallographie, RWTH Aachen.
[15] G. McIntyre, Program for calculating absorption, mean paths and extinction for single crystals TBAR, ILL Grenoble.
[16] V. Hutanu, M. Meven, G. Heger, Phys. B: Cond. Matter 397 (2007) 135–137; M. Meven, V. Hutanu, G. Heger, Neutron News 18 (2007) 19–21.
[17] G.M. Sheldrick, Acta Crystallogr. A 64 (2008) 112–122.
[18] D. Günther, R. Frischknecht, C.A. Heinrich, H.J. Kahlert, J. Anal. At. Spectrom. 12 (1997) 939–944.
[19] A. Schlechte, G. Auffermann, M. Bednarski, Ł. Bochenek, M. Böhme, T. Cichorek, R. Niewa, N. Oeschler, M. Schmidt, F. Steglich, R. Kniep, Chem. Phys. Chem. Submitted for Publication.
[20] R. Céolin, P. Khodadad, G. Sfez, J. Magn. Magn. Mater. 274 (1972) 1731–1734.
[21] R. Schmelczer, D. Schwarzenbach, Z. Naturforsch. 36b (1981) 463–469.
[22] A. Schlechte, R. Niewa, Yu. Prots, W. Schnelle, M. Schmidt, R. Kniep, Inorg. Chem. 48 (2009) 2277–2284.
[23] J. Schoenes, W. Bacsa, F. Hulliger, Solid State Commun. 68 (1988) 287–289.
[24] R.L. Withers, R. Vincent, J. Schoenes, J. Solid State Chem. 177 (2004) 701–708.